Extreme Mechanics Letters 39 (2020) 100797

Contents lists available at ScienceDirect

Extreme Mechanics Letters

journal homepage: www.elsevier.com/locate/eml

Synergy of noncovalent interlink and covalent toughener for tough hydrogel adhesion

Yecheng Wang [a], Dong Liang [b], Zhigang Suo [a,*], Kun Jia [b,*]

[a] John A. Paulson School of Engineering and Applied Sciences, Kavli Institute for Bionano Science and Technology, Harvard University, Cambridge, MA 02138, United States

[b] State Key Laboratory for Strength and Vibration of Mechanical Structures, School of Aerospace Engineering, Xi'an Jiaotong University, Xi'an 710049, China

ARTICLE INFO

Article history:
Received 26 February 2020
Received in revised form 19 May 2020
Accepted 29 May 2020
Available online 1 June 2020

Keywords:
Adhesion
Double-network hydrogel
Noncovalent interlink
Covalent toughener

ABSTRACT

Tough adhesion between soft and wet materials is important to many applications in medicine and engineering. Examples include implants, wound dressing, and soft machines. Recent work has highlighted a general principle: tough adhesion can be realized through the synergy of interlink and toughener. Here we develop an adhesive double-network hydrogel to achieve tough adhesion through noncovalent interlinks and covalent tougheners. We show that the noncovalent interlinks can be strong enough to unzip many covalent tougheners. Adhesion energy above 500 J/m^2 is achieved. Interplay between noncovalent interlinks and covalent tougheners provides new possibilities for toughening mechanism. This work will guide material designs for tough adhesion, as well as contribute to fundamental mechanics of adhesion.

1. Introduction

Since the 1960s, hydrogels have been developed for medical applications, including contact lenses, drug delivery, and tissue regeneration [1–3]. In more recent years, hydrogels have been used as stretchable, transparent, ionic conductors to enable unusual devices, such as soft machines [4–6], ionotronics [7–12], and noise cancellations [13]. Many tough hydrogels have been developed [3,14–18]. For example, when a double-network (DN) hydrogel is stretched, the short-chain network breaks over a substantial volume and the long-chain network remains intact, leading to high toughness (∼1000 J/m^2) [14,19]. In such a DN hydrogel, polymer chains of each network are crosslinked by covalent bonds. The hydrogel is chemically stable and fully swollen. The DN hydrogel resolves the stiffness-threshold conflict in single-network hydrogels: the short-chain network provides high stiffness, and the long-chain network provides high fatigue threshold [20]. The combined attributes of stability, stiffness, toughness, and fatigue resistance make the DN hydrogel promising for many applications.

Tough adhesion has been achieved recently between hydrogels and other materials, such as nonporous inorganics [21], elastomers [22], and living tissues [23]. Tough adhesion requires not only a tough hydrogel as dissipative matrix, but also strong interlinks. Diverse interlinks including covalent bonds [21–24], noncovalent bonds [25–27], and topological entanglement [28–30] have been developed. We have recently shown that noncovalent interlinks can be strong enough to unzip many noncovalent tougheners to achieve instant and tough adhesion [31]. So far, the DN hydrogel adhesion has been achieved only with a porous solid interface by in-situ polymerization [32]. Tough adhesion of pre-formed DN hydrogel has not been reported yet, but is potentially significant in antifouling coating, cartilage regeneration, and bioimplants [14,33].

Here we apply the synergy of interlink and toughener to design an adhesive DN hydrogel, which can strongly adhere to DN hydrogels with covalent tougheners through noncovalent interlinks. We show that noncovalent interlinks can be strong enough for many covalent tougheners to unzip. To illustrate the principle, we use chemically crosslinked poly(acrylic acid) (PAA) as the long-chain network and poly(2-acrylamido-2-methylpropane sulfonic acid) (PAMPS) as the short-chain network. Then, we adhere the PAMPS–PAA hydrogel to another DN hydrogel with the same covalent tougheners (PAMPS), but chemically crosslinked polyacrylamide (PAAM) as the long-chain network (Fig. 1). Hydrogen-bonding interlinks can form between carboxyl groups in PAA network and amide groups in PAAM network [31,34]. Although an individual hydrogen bond is weak, dense array of hydrogen bonds has been shown to be as strong as a covalent interlink. When an external force separates the adhesion, the covalent polymer networks transmit the force to the separation front. The interlinks need to be stronger than the tougheners,

* Corresponding authors.
E-mail addresses: suo@seas.harvard.edu (Z. Suo), kunjia@mail.xjtu.edu.cn (K. Jia).

https://doi.org/10.1016/j.eml.2020.100797
2352-4316/

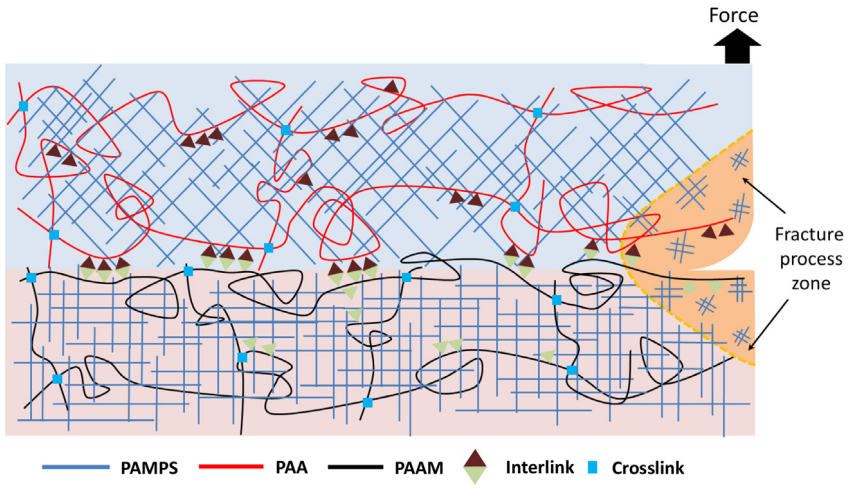

Fig. 1. Adhesive double-network hydrogel. The adhesive double-network hydrogel consists of two interpenetrating covalent networks: long-chain PAA network and short-chain PAMPS network. The PAMPS–PAA hydrogel adheres to a PAMPS–PAAM hydrogel through hydrogen bond formed between carboxyl groups in PAA and amide groups in PAAM. The PAMPS network serves as toughens in both hydrogels and ascertains the formation of dense array of hydrogen bonds at the interface due to its acidic nature. When an external force separates the adhesion, the force is transmitted by the covalent networks to the separation front. The crosslinks remain intact, but the toughens and interlinks unzip. The interlinks need to be strong enough to unzip many toughens. Along with the advance of separation, a process zone at the separation front dissipates energy.

so that many toughens unzip and dissipate energy, leading to tough adhesion. Along with the advance of the separation, a process zone at the separation front dissipates energy as the PAMPS network breaks.

The adhesion strongly depends on the amount of hydrogen bond formed at the interface [31]. PAA is a weak acid, with $pK_a = 4.5$ at room temperature. When $pH < pK_a$, more carboxyl groups are available to form hydrogen bond. The precursor of PAMPS has a pH of 0.6, and the precursor of PAA has a pH of 1.5, ensuring dense array of hydrogen bonds at the interface.

2. Material synthesis

We adopt an established two-step polymerization method [14] to fabricate the PAMPS–PAA hydrogel. As shown in Fig. 2, the first network was synthesized from an aqueous solution of 1M 2-acrylamido-2-methylpropanesulfonic acid (AMPS; Sigma-Aldrich, 818 667), 4 mol-% *N, N′*-methylenebisacrylamide(MBAA; Sigma-Aldrich, M7279), and 0.1 mol-% 2-oxoglutaric acid (OA; Sigma-Aldrich, 75 890) via UV photo-polymerization. In the argon gas environment, the prepared AMPS precursor was injected into a mold, which consists of two glass plates spaced by a 0.5 mm-thick U-shape silicone rubber. The mold with precursor was exposed to UV (15 W, 365 nm wavelength) for 8 h. Then, the PAMPS hydrogel was soaked in an aqueous solution of 4M acrylic acid (AA; Sigma-Aldrich, 147 230), 0.004 mol-% MBAA, and 0.1 mol-% OA for 24 h. Upon fully swollen, the sample was carefully sandwiched by two glass plates and coated with a transparent polyethylene membrane to avoid dehydration. The PAA network within the PAMPS network was subsequently synthesized by another 8-hour illumination under UV. The PAMPS–PAA hydrogel was soaked in deionized (DI) water for 48 h before use. The DI water was renewed every 8 h.

The synthesis of the PAMPS–PAAM hydrogel followed the same procedure as described above, with the same recipe: an aqueous solution of 4M acrylamide (AAM; Sigma-Aldrich, A8887), 0.004 mol-% MBAA, and 0.1 mol-% OA. The thickness of PAMPS–PAA hydrogel and PAMPS–PAAM hydrogel are 1.25 mm and 1.65 mm, respectively.

3. Mechanical properties of PAMPS-PAA hydrogel

The as-prepared PAMPS–PAA hydrogel wih dumbbell-shape was loaded by a tensile machine (SHIMADZU AGS-X) for uniaxial tensile test The loading rate was 100 mm/min. Five samples were tested. To compare, we also tested five PAMPS–PAAM hydrogel samples (Fig. 3a and b). Each sample has an effective length of 12 mm and a width of 2 mm. The nominal stress is the force divided by the initial cross-section area. Before rupture, the measured nominal stress at each stretch shows good consistence for all the PAMPS–PAA and PAMPS–PAAM samples. The stress–stretch curves of PAMPS–PAA hydrogel and PAMPS–PAAM hydrogel show rather different behaviors. PAMPS–PAAM hydrogel is more stretchable and has noticeable strain stiffening, while PAMPS–PAA hydrogel yields at a stretch smaller than 3 and ruptures subsequently. Since the elasticity of DN hydrogels mainly depends on the long-chain network, the difference in stress–stretch curve indicates the difference between PAAM and PAA in stretchability. It is noticed that the maxmium stretch of one PAMPS–PAA sample reaches 4.5. During this process, necking happens sequentially on two sections of the sample. A possible explanation is the more serious inhomogeneity of PAMPS–PAA hydrogel. When a DN hydrogel is stretched to certain amount, necking is observed [35]. If the DN hydrogel is stretched more, more PAMPS clusters are created. These clusters increase the inhomogeneity of the hydrogel and serve as physical crosslink [19, 36]. Therefore, the variation in stress–stretch curve among samples is large.

Fig. 3c shows the averaged modulus of both hydrogels in small-strain status. The early stage of the stress–stretch curves is used for fitting to the neo-Hookean model:

$$W = \frac{1}{2}\mu(\lambda_1^2 + \lambda_2^2 + \lambda_3^2 - 3), \tag{1}$$

where W is the Helmholtz energy density, $\lambda_{1,2,3}$ are the principal stretches, and μ is the shear modulus. As λ_1 is prolonged in uniaxial stretch and the hydrogel is taken to be incompressible, we have $\lambda_2 = \lambda_3 = 1/\sqrt{\lambda_1}$. The nominal stress s_1 is derived by the derivation of W to the principle stretch λ_1:

$$s_1 = \mu(\lambda_1 - \lambda_1^{-2}). \tag{2}$$

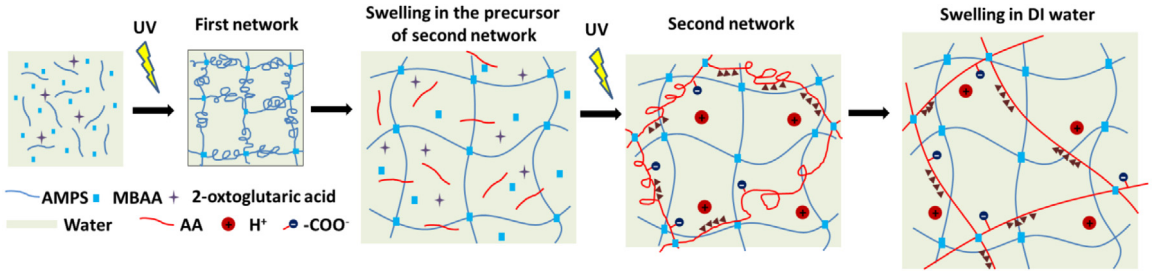

Fig. 2. Two-step polymerization method for the synthesis of the PAMPS–PAA hydrogel. An aqueous solution of 1M AMPS, 4 mol-% MBAA, and 0.1 mol-% OA was prepared. In the argon gas environment, the AMPS precursor solution was injected into a mold sandwiched by two glass plates and exposed to UV for 8 h. The first network was then soaked in an aqueous solution of 4M AA, 0.004 mol-% MBAA, and 0.1 mol-% OA for 24 h to reach a fully swollen state. After that the sample sandwiched by two glass plates was exposed to UV for 8 h. Last, the synthesized PAMPS–PAA hydrogel was soaked in deionized (DI) water for 48 h to remove the residual reactants.

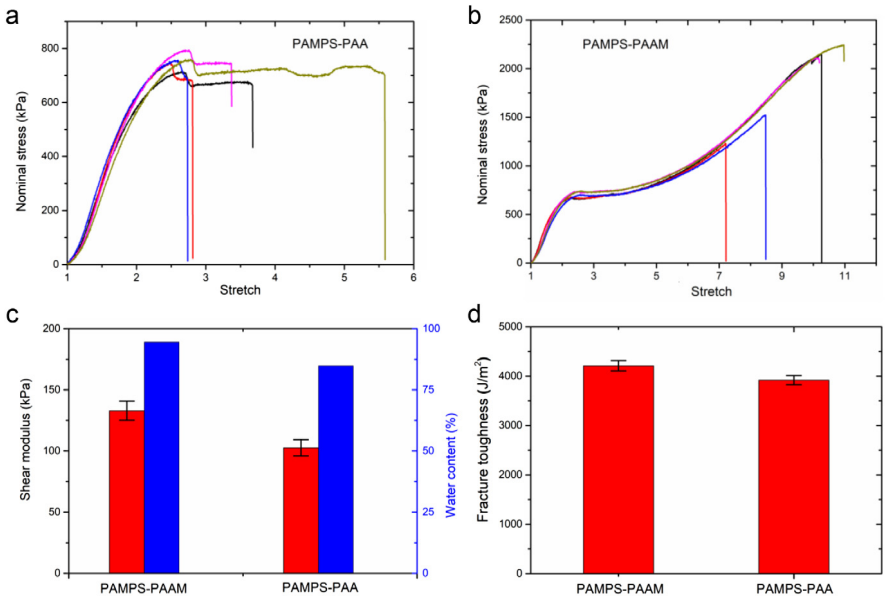

Fig. 3. Mechanical properties of the PAMPS–PAA hydrogel and the comparisons to PAMPS–PAAM hydrogel. Unless otherwise specified, the PAMPS–PAA hydrogel and the PAMPS–PAAM are fully swollen and have a thickness of 1.25 mm and 1.65 mm, respectively. (a) Nominal stresss vs stretch of PAMPS–PAA. (b) Nominal stress vs stretch of PAMPS–PAAM. (c) Shear modulus and water concentration of PAMPS–PAAM and PAMPS–PAA. (d) Toughness of PAMPS–PAAM and PAMPS–PAA, measured by pure shear test.

For the linear section of the stress–stretch curve, λ_1 is around 1, and the above equation can be simplified to $s_1 = 3\mu(\lambda_1 - 1)$. The initial slope of the stress–stretch curve is three times the shear modulus. Since the PAMPS network contributes to the stiffness, PAMPS–PAA and PAMPS–PAAM have similar Young's modulus, so as the measured water content (Fig. 3c). In addition, we measure the toughness of the DN hydrogels by pure shear test (Figs. 3d and 4). Although the stretchabilities of the synthesized DN hydrogels vary a lot, the PAMPS–PAA hydrogel and PAMPS–PAAM hydrogel have similar toughness of about 4000 J/m^2.

We use pure shear test to measure the fracture toughness (Fig. 4), where a notched sample and an unnotched sample are required. Accordingly, two sets of samples are prepared from the same piece of DN hydrogel with the same geometry, 50 mm $\times$10 mm. For the notched sample, a pre-cut crack with 20 mm length is introduced (Fig. 4a and b). Both of the notched and unnotched samples are subjected to a monotonic stretch until rupture. The loading rate is 30 mm/min. For static fracture, the measurement of one sample only takes several minutes, so the samples are exposed to open air. Stress–stretch curves of the notched and unnotched samples are measured for PAMPS–PAAM with 1.65 mm thickness (Fig. 4c and d) and PAMPS–PAA with 1.25 mm thickness (Fig. 4e and f). The stretch limit λ_c at which the crack starts to propagate is recorded and used to calculate the fracture toughness. According to the definition of fracture toughness, the critical energy release rate for crack propagation is calculated by the integration of stress–stretch below λ_c (Fig. 4d and f). For each measurement, three samples are tested.

4. Adhesion energy

We measure the adhesion energy between PAMPS–PAA hydrogel and PAMPS–PAAM hydrogel by 90-degree peel test (Fig. 5a). The prepared 1.65 mm thick PAMPS–PAAM hydrogel and 1.25 mm thick PAMPS–PAA hydrogel were cut into rectangular samples with a length of 100 mm and a width of 2 mm. The PAMPS–PAAM was glued to a rigid acrylic substrate using cyanoacrylate (superglue), while PAMPS–PAA was glued to a 50-μm thick polyethylene terephthalate (PET) film as inextensible backing layer. The increment in the pull distance equals the extension of the crack in the steady state. The acrylic substrate and PET film were washed with ethanol and DI water, then dried before use. Since both PAMPS–PAA hydrogel and PAMPS–PAAM hydrogel are acidic, the surfaces were treated with a few drops of 0.1 mol/L $NaHCO_3$ solution for 5 min and then dried before applying super glue. A small piece of PET film was inserted to the interface of

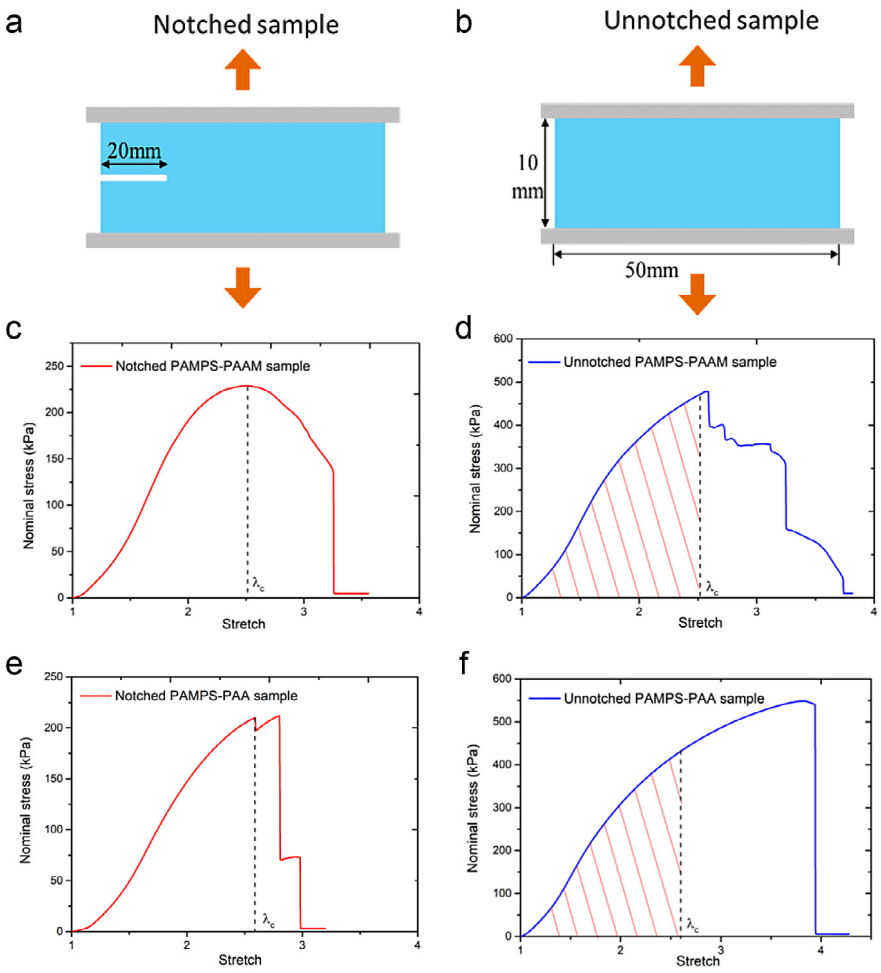

Fig. 4. Pure shear test for fracture toughness measurement. (a) Notched sample and (b) unnotched sample are subject to a monotonic stretch. (c) Stress–stretch curve of the notched PAMPS–PAAM. The stretch limit λ_c is recorded. (d) Stress–stretch curve of the unnotched PAMPS–PAAM. The fracture toughness equals to the product of the area enclosed by the stress–stretch curve of the unnotched PAMPS–PAAM at the stretch limit λ_c and the thickness. (e) Stress–stretch curve of the notched PAMPS–PAA. (f) Stress–stretch curve of the unnotched PAMPS–PAA.

the two hydrogels to introduce a pre-crack. The PAMPS–PAA and PAMPS–PAAM samples were made into contact and a weight of 1 kg was applied for 5 min before test. The loading rate was 100 mm/min. The adhesion energy was calculated by the average force at the plateau of the force–displacement curve divided by the sample width.

After peel, no hydrogel residues are observed on the surfaces of the hydrogels, indicating an adhesion failure mode. As shown in Fig. 5b, the adhesion energy between PAMPS–PAA and PAMPS–PAAM exceeds 500 J/m^2. By contrast, the adhesion energy between PAA and PAMPS–PAAM is about 180 J/m^2, which is comparable to the fracture toughness of PAA [31]. It means that the interlinks are strong enough and the adhesion is limited by the brittleness of PAA. The viscoelasticity of PAA has been shown to be negligible [31]. It corroborates that the adhesion originates from the interlinks on the interface. The force–displacement curves of the adhesion between PAMPS–PAA and PAMPS–PAAM and the adhesion between PAA and PAMPS–PAAM are shown in Fig. 5c and d, respectively.

5. Discussion and conclusion

Tough adhesion is analogous to tough hydrogel. Besides the hydrogel matrix with toughener used as adhesive and/or adherend, it incorporates an additional player: interlink on the interface. Achieving tough adhesion requires not only the synergy of elastic network and tougheners, but also the cooperation of interlinks. When a force separates the adhesion, the strechable polymer network in the adhesive and/or the adherend transmits the force through the bulk matrix to the separation front, which concentrates stress. For weak interlinks, they unzip, but the tougheners remain zipped. So, strong interlinks are essential to elicit the energy dissipation process. The diversity of covalent and noncovalent bonds provides enormous design space to realize tough adhesion. Table 1 summarizes the available methods. It is well known that the dissociation energy of noncovalent bond, such as ionic interaction (42–82 kJ/mol), hydrogen bond (12–29 kJ/mol), and hydrophobic association, is much lower than that of covalent bond (several hundred kJ/mol) [33]. Covalent interlinks and non covalent bonds inside the matrix as tougheners are firstly selected to design a tough hydrogel adhesion [21–23,37]. For this family of adhesives, the reaction between primary amine groups and carboxylic acid groups under the coupling reagents is commonly used to form covalent interlinks on the interface. When a force separates the adhesion, a number of tougheners formed by the ligands-Ca^{2+} group or hydrogen bond unzip before the covalent interlinks break.

Replacing slowly formed covalent interlinks with noncovalent interlinks is more convenient for time-sensitive applications, such as wound closure, bio-implants, and rapid prototyping. As the strength of three players (i.e., hydrogel matrix, toughener, and interlink) relates to not only the energy of a single bond, but also

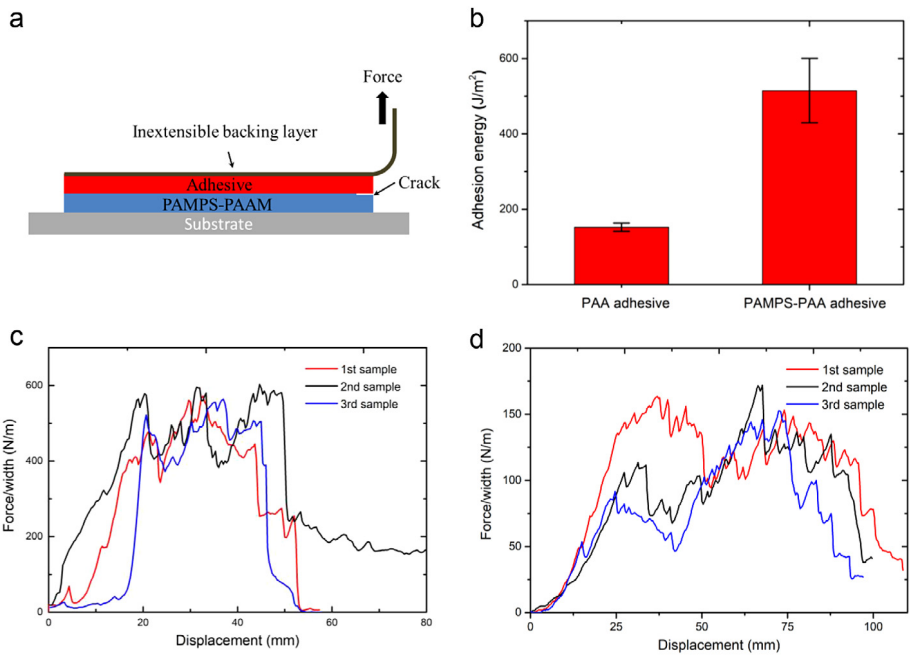

Fig. 5. Adhesion measurement. (a) Experimental setup of the 90-degree peel test. (b) Adhesion energy between PAA and PAMPS–PAAM and that between PAMPS–PAA and PAMPS–PAAM. (c) Force–displacement curves of the adhesion between PAMPS–PAA and PAMPS–PAAM. (d) Force–displacement curves of the adhesion between PAA and PAMPS–PAAM. Three samples are used for each test.

Table 1
Examples of tough hydrogel adhesion.

		Interlink	
		Covalent bond	Noncovalent bond
Toughener	Covalent bond	NA	This work
	Noncovalent bond	Li, et al. [23], Yuk, et al. [21,22,37], Liu et al. [24]	① Yang, et al [28] Gao, et al. [29] ② Wang, et al. [31], Shen, et al. [38] ③ Roy,et al [39], Xu, et al. [40]

① Topological interlink; ② interlink on stretchable network; ③ interlink on sacrificial network.

the number of bond, various noncovalent interlinks (e.g., hydrogen bond, π-π stacking, metal complexation, and hydrophobic interaction) have been widely used to unzip noncovalent tougheners [28,31]. Generally, this method includes three types. One is topological adhesion incorporating additional stitching polymers to form the interlinks [28,29]. The other two are direct formations of interlinks by the functional groups on the stretchable [31,38] or sacrificial network [39,40] of the hydrogel matrix. Our previous study has demonstrated that hydrogen bond can be strong enough to unzip ionic tougheners [31]. Here, we have successfully filled the blank of Table 1 labeled with noncovalent interlink and covalent toughener. However, tough hydrogel adhesion via covalent interlinks between hydrogels with covalent tougheners has not been demonstrated so far.

In conclusion, we have designed an adhesive double-network hydrogel to achieve tough adhesion through noncovalent interlinks. We show that noncovalent interlinks can be strong enough for many covalent tougheners to unzip by adhering the adhesive double-network hydrogel to another double-network hydrogel with covalent tougheners. Adhesion energy above 500 J/m^2 has been reached. This work broadens the strategies of energy dissipation for tough adhesion.

Declaration of competing interest

The authors declare that they have no known competing financial interests or personal relationships that could have appeared to influence the work reported in this paper.

Acknowledgment

This work is supported by the National Natural Science Foundation of China (Grant No. 11872292 and 11732012). Y.W. and Z.S. acknowledge the support of NSF MRSEC, United States (DMR-14-20570).

References

[1] O. Wichterle, D. Lím, Hydrophilic gels for biological use, Nature 185 (1960) 117–118, http://dx.doi.org/10.1038/185117a0.
[2] K.Y. Lee, D.J. Mooney, Hydrogels for tissue engineering, Chem. Rev. 101 (2001) 1869–1880, http://dx.doi.org/10.1021/cr000108x.
[3] Y.S. Zhang, A. Khademhosseini, Advances in engineering hydrogels, Science 356 (2017) eaaf3627, http://dx.doi.org/10.1126/science.aaf3627.
[4] E. Acome, S.K. Mitchell, T.G. Morrissey, M.B. Emmett, C. Benjamin, M. King, M. Radakovitz, C. Keplinger, Hydraulically amplified self-healing electrostatic actuators with muscle-like performance, Science 359 (2018) 61–65, http://dx.doi.org/10.1126/science.aao6139.
[5] B. Chen, J.J. Lu, C.H. Yang, J.H. Yang, J. Zhou, Y.M. Chen, Z. Suo, Highly stretchable and transparent ionogels as nonvolatile conductors for dielectric elastomer transducers, ACS Appl. Mater. Interfaces 6 (2014) 7840–7845, http://dx.doi.org/10.1021/am501130t.
[6] T. Li, G. Li, Y. Liang, T. Cheng, J. Dai, X. Yang, B. Liu, Z. Zeng, Z. Huang, Y. Luo, T. Xie, W. Yang, Fast-moving soft electronic fish, Sci. Adv. (2017) 8.
[7] J.-Y. Sun, C. Keplinger, G.M. Whitesides, Z. Suo, Ionic skin, Adv. Mater. 26 (2014) 7608–7614, http://dx.doi.org/10.1002/adma.201403441.
[8] C.-C. Kim, H.-H. Lee, K.H. Oh, J.-Y. Sun, Highly stretchable, transparent ionic touch panel, (n.d.) 7.
[9] H.-R. Lee, C.-C. Kim, J.-Y. Sun, Stretchable ionics - A promising candidate for upcoming wearable devices, Adv. Mater. 30 (2018) 1704403, http://dx.doi.org/10.1002/adma.201704403.

[10] C. Yang, Z. Suo, Hydrogel ionotronics, Nat. Rev. Mater. 3 (2018) 125–142, http://dx.doi.org/10.1038/s41578-018-0018-7.
[11] C. Keplinger, J.-Y. Sun, C.C. Foo, P. Rothemund, G.M. Whitesides, Z. Suo, Stretchable, transparent, ionic conductors, Science 341 (2013) 984–987, http://dx.doi.org/10.1126/science.1240228.
[12] S.Z. Bisri, S. Shimizu, M. Nakano, Y. Iwasa, Endeavor of iontronics: From fundamentals to applications of ion controlled electronics, Adv. Mater. 29 (2017) 1607054, http://dx.doi.org/10.1002/adma.201607054.
[13] P. Rothemund, X.P. Morelle, K. Jia, G.M. Whitesides, Z. Suo, A transparent membrane for active noise cancelation, Adv. Funct. Mater. 28 (2018) 1800653, http://dx.doi.org/10.1002/adfm.201800653.
[14] J.P. Gong, Y. Katsuyama, T. Kurokawa, Y. Osada, Double-network hydrogels with extremely high mechanical strength, Adv. Mater. 15 (2003) 1155–1158, http://dx.doi.org/10.1002/adma.200304907.
[15] X. Zhao, Multi-scale multi-mechanism design of tough hydrogels: building dissipation into stretchy networks, Soft Matter. 10 (2014) 672–687, http://dx.doi.org/10.1039/C3SM52272E.
[16] J.-Y. Sun, X. Zhao, W.R.K. Illeperuma, O. Chaudhuri, K.H. Oh, D.J. Mooney, J.J. Vlassak, Z. Suo, Highly stretchable and tough hydrogels, Nature 489 (2012) 133–136, http://dx.doi.org/10.1038/nature11409.
[17] R. Long, C.-Y. Hui, Crack tip fields in soft elastic solids subjected to large quasi-static deformation — A review, Extreme Mech. Lett. 4 (2015) 131–155, http://dx.doi.org/10.1016/j.eml.2015.06.002.
[18] C.W. Peak, J.J. Wilker, G. Schmidt, A review on tough and sticky hydrogels, Colloid Polym. Sci. 291 (2013) 2031–2047, http://dx.doi.org/10.1007/s00396-013-3021-y.
[19] J.P. Gong, Why are double network hydrogels so tough? Soft Matter. 6 (2010) 2583, http://dx.doi.org/10.1039/b924290b.
[20] Y. Zhou, W. Zhang, J. Hu, J. Tang, C. Jin, Z. Suo, T. Lu, The stiffness-threshold conflict in polymer networks and a resolution, J. Appl. Mech. 87 (2020) 031002, http://dx.doi.org/10.1115/1.4044897.
[21] H. Yuk, T. Zhang, S. Lin, G.A. Parada, X. Zhao, Tough bonding of hydrogels to diverse non-porous surfaces, Nature Mater. 15 (2016) 190–196, http://dx.doi.org/10.1038/nmat4463.
[22] H. Yuk, T. Zhang, G.A. Parada, X. Liu, X. Zhao, Skin-inspired hydrogel–elastomer hybrids with robust interfaces and functional microstructures, Nature Commun. 7 (2016) 12028, http://dx.doi.org/10.1038/ncomms12028.
[23] J. Li, A.D. Celiz, J. Yang, Q. Yang, I. Wamala, W. Whyte, B.R. Seo, N.V. Vasilyev, J.J. Vlassak, Z. Suo, D.J. Mooney, Tough adhesives for diverse wet surfaces, Science 357 (2017) 378–381, http://dx.doi.org/10.1126/science.aah6362.
[24] Q. Liu, G. Nian, C. Yang, S. Qu, Z. Suo, Bonding dissimilar polymer networks in various manufacturing processes, Nature Commun. 9 (2018) 846, http://dx.doi.org/10.1038/s41467-018-03269-x.
[25] H. Yi, S.H. Lee, M. Seong, M.K. Kwak, H.E. Jeong, Bioinspired reversible hydrogel adhesives for wet and underwater surfaces, J. Mater. Chem. B 6 (2018) 8064–8070, http://dx.doi.org/10.1039/C8TB02598C.
[26] D. Gan, W. Xing, L. Jiang, J. Fang, C. Zhao, F. Ren, L. Fang, K. Wang, X. Lu, Plant-inspired adhesive and tough hydrogel based on Ag-Lignin nanoparticles-triggered dynamic redox catechol chemistry, Nature Commun. 10 (2019) 1487, http://dx.doi.org/10.1038/s41467-019-09351-2.
[27] S. Rose, A. Prevoteau, P. Elzière, D. Hourdet, A. Marcellan, L. Leibler, Nanoparticle solutions as adhesives for gels and biological tissues, Nature 505 (2014) 382–385, http://dx.doi.org/10.1038/nature12806.
[28] J. Yang, R. Bai, Z. Suo, Topological adhesion of wet materials, Adv. Mater. 30 (2018) 1800671, http://dx.doi.org/10.1002/adma.201800671.
[29] Y. Gao, K. Wu, Z. Suo, Photodetachable adhesion, Adv. Mater. (2018) 1806948, http://dx.doi.org/10.1002/adma.201806948.
[30] J. Yang, R. Bai, J. Li, C. Yang, X. Yao, Q. Liu, J.J. Vlassak, D.J. Mooney, Z. Suo, Design molecular topology for wet–dry adhesion, ACS Appl. Mater. Interfaces 11 (2019) 24802–24811, http://dx.doi.org/10.1021/acsami.9b07522.
[31] Y. Wang, K. Jia, C. Xiang, J. Yang, X. Yao, Z. Suo, Instant, tough, noncovalent adhesion, ACS Appl. Mater. Interfaces 11 (2019) 40749–40757, http://dx.doi.org/10.1021/acsami.9b10995.
[32] T. Kurokawa, H. Furukawa, W. Wang, Y. Tanaka, J.P. Gong, Formation of a strong hydrogel–porous solid interface via the double-network principle, Acta Biomater. 6 (2010) 1353–1359, http://dx.doi.org/10.1016/j.actbio.2009.10.046.
[33] Q. Chen, H. Chen, L. Zhu, J. Zheng, Fundamentals of double network hydrogels, J. Mater. Chem. B 3 (2015) 3654–3676, http://dx.doi.org/10.1039/C5TB00123D.
[34] G. Sudre, L. Olanier, Y. Tran, D. Hourdet, C. Creton, Reversible adhesion between a hydrogel and a polymer brush, Soft Matter. 8 (2012) 8184, http://dx.doi.org/10.1039/c2sm25868d.
[35] Y.-H. Na, Y. Tanaka, Y. Kawauchi, H. Furukawa, T. Sumiyoshi, J.P. Gong, Y. Osada, Necking phenomenon of double-network gels, Macromolecules 39 (2006) 4641–4645, http://dx.doi.org/10.1021/ma060568d.
[36] Y. Kawauchi, Y. Tanaka, H. Furukawa, T. Kurokawa, T. Nakajima, Y. Osada, J.P. Gong, Brittle, ductile, paste-like behaviors and distinct necking of double network gels with enhanced heterogeneity, J. Phys.: Conf. Ser. 184 (2009) 012016, http://dx.doi.org/10.1088/1742-6596/184/1/012016.
[37] H. Yuk, C.E. Varela, C.S. Nabzdyk, X. Mao, R.F. Padera, E.T. Roche, X. Zhao, Dry double-sided tape for adhesion of wet tissues and devices, Nature 575 (2019) 169–174, http://dx.doi.org/10.1038/s41586-019-1710-5.
[38] M. Shen, L. Li, Y. Sun, J. Xu, X. Guo, R.K. Prud'homme, Rheology and adhesion of poly(acrylic acid)/laponite nanocomposite hydrogels as biocompatible adhesives, Langmuir 30 (2014) 1636–1642, http://dx.doi.org/10.1021/la4045623.
[39] C.K. Roy, H.L. Guo, T.L. Sun, A.B. Ihsan, T. Kurokawa, M. Takahata, T. Nonoyama, T. Nakajima, J.P. Gong, Self-adjustable adhesion of polyampholyte hydrogels, Adv. Mater. 27 (2015) 7344–7348, http://dx.doi.org/10.1002/adma.201504059.
[40] J. Xu, G. Wang, Y. Wu, X. Ren, G. Gao, Ultrastretchable wearable strain and pressure sensors based on adhesive, tough, and self-healing hydrogels for human motion monitoring, ACS Appl. Mater. Interfaces 11 (2019) 25613–25623, http://dx.doi.org/10.1021/acsami.9b08369.